Multimodal Cardiovascular Information Monitor Using Piezoelectric Transducers for Wearable Healthcare

Okano, Takaaki
Izumi, Shintaro
Katsuura, Takumi
Kawaguchi, Hiroshi
Yoshimoto, Masahiko

Multimodal Cardiovascular Information Monitor Using Piezoelectric Transducers for Wearable Healthcare

Takaaki Okano[1], Shintaro Izumi[2], Takumi Katsuura[1], Hiroshi Kawaguchi[1], and Masahiko Yoshimoto[1]

***Abstract*—This article describes a multimodal cardiovascular information measurement method using a wearable device composed of piezoelectric transducers. Cardiovascular diseases are increasing with the aging population, and they constitute a significant portion of the causes of death and long-term care. In recent years, daily-life monitoring using wearable sensor devices has attracted particular attention for the prevention and early detection of cardiovascular diseases. However, recent wearable devices can only measure limited cardiovascular information such as the heart rate. In contrast, the proposed method can simultaneously measure heart rate variability, pulse wave propagation velocity, and blood flow velocity using only a piezoelectric transducer array.**

***Keywords*—blood flow velocity; sensor array; piezoelectric transducer; pulse wave; ultra sound; wearable sensor**

I. INTRODUCTION

The increase in medical cost owing to the increase in patients with noncommunicable diseases (NCDs) has been a critical issue worldwide. Four primary types of NCDs are cardiovascular diseases, cancers, chronic respiratory diseases, and diabetes. World Health Organization (WHO) reported that NCDs kill 38 million people in the world annually. Smoking, physical inactivity, unhealthy diet, and excessive alcohol consumption can increase the risk of NCDs. To protect ourselves against NCDs, our lifestyle quality must be improved.

Proper daily exercise and physical activity are important for mitigating and forestalling NCDs. For the efficient management of exercise, recording daily physical information and analyzing it in real time are important. Wearable devices are convenient for monitoring and recognizing biosignals and physical activities in daily life. Long-term biosignal monitoring using wearable devices can also contribute to the early detection of NCDs.

This study focuses on cardiovascular information monitoring using a wearable device. In recent years, various wearable devices have been developed to measure biological signals. We can recognize fluctuations in the indicators and abnormal values using long-term monitoring in daily life. Wristwatch-type heart rate monitors using photoplethysmography (PPG) are typically used. A lot of recent wearable devices is investigated in literatures [1–4]. As shown in these literatures, the latest wearable devices tend to have multimodal sensing capability. However, biological signals that can be measured by these devices are limited: electrocardiogram (ECG), pulse wave, SpO2, temperature, and respiration.

We herein propose a wearable device that can measure cardiovascular indices different from conventional ones. Fig. 1 presents the concept of the proposed device; it can simultaneously measure heart rate variation, pulse wave propagation speed, and blood flow velocity. These various indices can contribute to the early detection and prevention of cardiovascular diseases.

The proposed method uses a device having multiple piezoelectric transducers. Subsequently, the pressure pulse wave is measured at multiple positions of the wrist. Simultaneously, ultrasound waves are transmitted toward the body surface and reflected waves from body tissues are measured (see Fig. 1). Because the pulse wave and the ultrasound wave have different frequency ranges, they can be measured simultaneously using the same piezoelectric transducer. The pulse wave velocity can be extracted from the arrival time difference of piezoelectric pulse waves, which are measured at multiple locations. The reflected ultrasound wave from the blood vessel changes its center frequency according to the blood flow velocity because of the Doppler effect.

This paper is structured as follows. The significance and

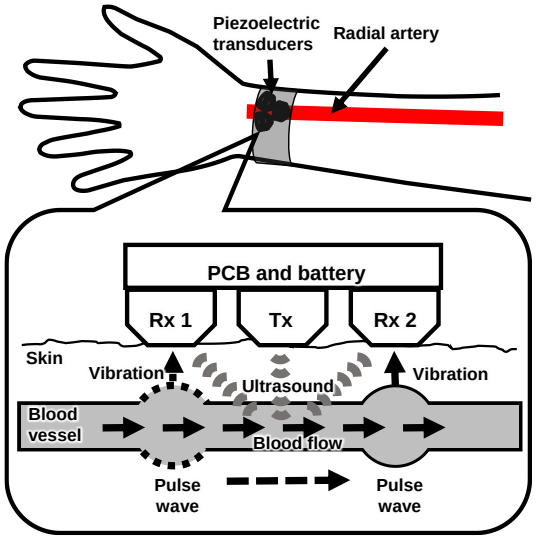

Figure 1 Concept design of proposed device using piezoelectric transducers array.

1. Graduate School of System Informatics, Kobe University, 1-1 Rokkodai, Nada, Kobe, Hyogo 657-8501 Japan.
2. Institute of Scientific and Industrial Research, Osaka University, 8-1 Mihogaoka, Ibaraki, Osaka 567-0047, Japan.

This research was supported by JSPS KAKENHI Grant Number JP16H05868.

application of the biological signal measured by the proposed method are described in Section II. The details of the respective measurement methods are presented in Section III. The measurement results are shown in Section IV.

II. CardiovasculAr Information and Conventional Measurement Methods

A. Heart Rate Variation

The heart rate is a beat interval of the heart, and it includes various information related to human health. For example, the Karvonen Formula [5] can be used for calculating the strength of aerobic exercise from the relation between the average heart rate and the normal heart rate. The heart rate can also be used for heart rate variation analysis (HRVA). HRVA analyzes the fluctuation of the heart rate and its frequency characteristics to monitor stress conditions and the precursor detection of cardiac diseases [6]. However, an instantaneous heartbeat interval at every beat is required for HRVA instead of the average heartbeat interval.

Generally, an ECG or PPG is used to measure the heartbeat. ECG measures the potential difference on the body surface attributable to the electrical activity of the heart. The PPG sensor irradiates green or red light to the body surface and measures the amount of light absorption by the hemoglobin related to the volume change in blood vessels. The heartbeat interval is obtained by detecting the peak from the waveform of these biological signals.

A pressure pulse wave can also be used for heartbeat measurement. It is measured by placing an acceleration sensor or a pressure sensor on the skin surface close to the artery (e.g., radial artery or carotid artery). We chose the pressure pulse wave in the proposed scheme.

B. Pulse Wave Velocity (PWV)

A pulse wave is generated by the heart and it propagates to the end region, such as limbs. Subsequently, the pulse wave velocity (PWV) is affected by the blood vessel hardness, the blood vessel wall thickness, and the blood pressure. For example, the increase in PWV is shown as arteriosclerosis progresses. Its correlation with the blood pressure has also attracted attention and a cuff-less blood pressure estimation method using PWV has been proposed [7]. Furthermore, it is related to the mental state. It has been indicated that depressed patients who consider suicide exhibit fluctuating PWVs [8].

The PWV is obtainable from the difference in the pulse wave arrival times and the distance of the pulse wave sensors, and is measured at two or more points of the body surface. In general, it is measured using two or more devices or probes (e.g., pulse waves measured at wrist and ankle, or ECG and pulse wave measured at fingertip).

C. Blood Flow Verocity

The blood flow velocity is a different index from the PWV. The PWV is obtained from the oscillation (pulse wave) of the blood vessel wall accompanied by the pulsation. Meanwhile, the blood flow velocity represents the speed at which the blood flows through the blood vessels. Blood flow velocity is used as an index of arterial disease such as arterial occlusion. The relation between lifestyle habits and the fluctuation of the blood flow velocity in peripheral blood vessel has been studied [9].

To measure the blood flow velocity from the body surface, an ultrasound wave is generally used. The ultrasound wave is irradiated from the body surface, and its reflected wave from the blood flowing through the blood vessel is measured. Because the center frequency of the reflected wave is changed by the Doppler effect according to the blood flow velocity, the velocity is obtainable from the frequency shift amount.

III. Proposed Multimodal Cardiovascular Information Measurement Method

To acquire the multimodal cardiovascular information described above with the wearable device, this study proposes the simultaneous measurement method using multiple piezoelectric elements and the ultrasound wave. The radial artery of the wrist, or the carotid artery of the neck is assumed as the measurement site.

Figs. 2 and 3 portray the overall block diagram of the proposed system and the blood flow velocity measurement method using piezoelectric transducers, respectively. The piezoelectric transducer has a 40-kHz resonance frequency. Although conventional blood flow velocimeters or diagnostic ultrasound imaging systems use the MHz band ultrasound, a lower frequency band is chose in this study to reduce the power consumption of circuits. A circular piezoelectric ceramic is placed inside the housing. A silicone of 1 mm thickness is sandwiched between the transceiver of the front face of the housing and the skin to mitigate the difference in

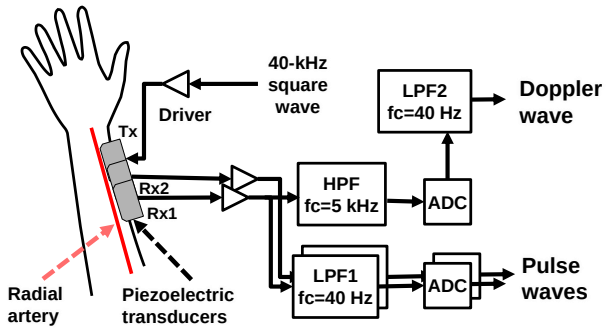

Figure 2 Block diagram of proposed sensor.

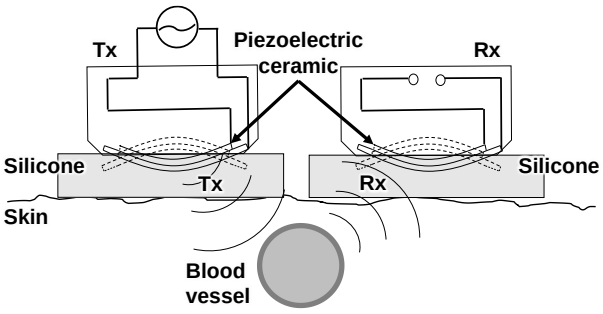

Figure 3 Reflection wave measurement method using piezoelectric transducers. Center frequency of reflection wave is shifted by Doppler effect.

the dielectric constant.

A. *Simultaneous Recording of Pulse Wave and Reflected Ultrasound Wave*

The reflected ultrasound wave and vibrations in blood vessels attributable to the pulsation of the heart are measured simultaneously using a piezoelectric transducer. Information related to the blood flow velocity is included in the reflected ultrasound wave because of the Doppler effect. The vascular vibrations caused by pulsation also include the pulse wave information.

The output signal of the receiver using the piezoelectric transducer includes both the pulse wave component and the reflected ultrasound wave component, as shown in Fig. 4(a). The pulse wave component exists in the low-frequency range of 1–30 Hz. The reflected ultrasound wave including the blood flow velocity information exists in the high-frequency range of approximately 40 kHz. A hum noise generated by an AC power supply is also included in the received signal.

Fig. 4 shows a separation processing flow for the reflected wave and the pulse wave. A high-pass filter with 5-kHz cutoff frequency and a low-pass filter with 40-Hz cutoff frequency are used for the separation. Subsequently, the reflected wave is mixed by the 40-kHz signal, which is transmitted as ultrasound, to convert its center frequency. As shown in Fig. 2, only the AD converter with 40-kHz sampling rate is used for mixing in this study. When the out-of-band signals are sufficiently filtered, the mixing can be realized by aliasing the AD converter. Finally, only the frequency component shifted by the Doppler effect is extracted from a low-pass filter with 40-Hz cutoff frequency.

The extracted pulse wave is a pressure pulse wave. It is more susceptible to noise, such as body movements, than ECG or PPG, as presented in Fig. 5. To extract an accurate heart beat interval from a pulse wave with low SNR, the autocorrelation [10] of the pulse wave is calculated. Because this method exploits the waveform similarity, it becomes more resistant to noise than simply calculating the time difference of the waveform peaks..

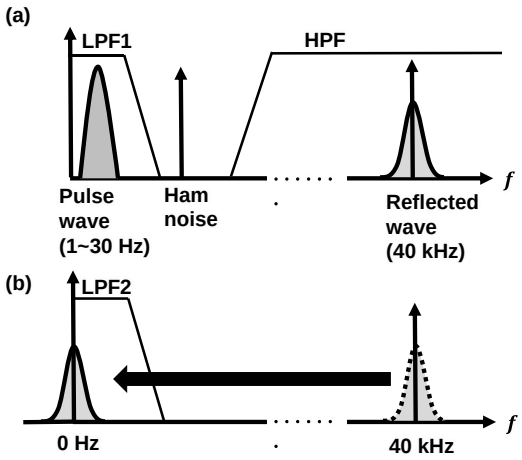

Figure 4 Separation flow of reflected ultrasound wave and pulse wave. (a) frequency characteristics of received signal and (b) frequency conversion of ultrasound wave by mixiing.

B. *Analysis of Blood Flow Velocity from Reflected Wave*

Ultrasound is a sound with a higher frequency than the human audible range of 20 Hz–20 kHz. Because the ultrasound wave is a propagation of vibration, it cannot be transmitted in vacuum. The propagation speed depends on the hardness and density of the medium, and it is independent of the frequency. The propagation speed is generally 340 m/s in air and 1530 m/s in vivo.

When an ultrasound wave propagates from a medium to a different medium, reflected waves and passing waves are generated. The ratio of reflection to passage is determined by the difference in the characteristic acoustic impedance at the boundary of the medium. The characteristic acoustic impedance defined as (1) expresses the acoustic property of a substance.

$$z = \rho \times c \quad \textbf{(1)}$$

Here, z, ρ, and c denote the characteristic acoustic impedance [kg/(m^{2}s)] , density of a medium[kg/(m^3)], and acoustic velocity in the medium [m/s], respectively. Consequently, reflectance R is expressed by (2).

$$R = \frac{Z2 - Z1}{Z2 + Z1} \quad \textbf{(2)}$$

Therein, Z1 and Z2 are the characteristic acoustic impedances of the incident side and transmission side

The characteristic acoustic impedance in air and in vivo are 0.0004×10^6 [kg/(m^{2}s)] and $1.52–1.68\times10^6$ [kg/(m^{2}s)], respectively. Consequently, the reflectance R is 0.9994–0.9995. Most of the waves are reflected when air exists between the piezoelectric transducer and the human body. To prevent the reflection caused by air, the proposed device uses soft silicone rubber between the human body and the piezoelectric transducer, as shown in Fig. 3. The specific acoustic impedance of silicone rubber is 1.2×10^6 [kg/(m^{2}s)] [11]. Subsequently, the reflectance at the boundary between

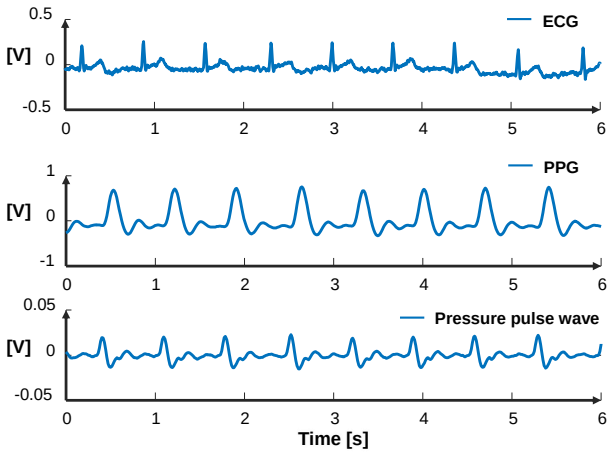

Figure 5 Measured examples of ECG, PPG, and pressure pulse wave using proposed method with piezoerectric transducer. ECG and PPG are simultaneously measured using reference sensors.

the silicone and the living body is 0.12–0.16.

When the ultrasound wave is irradiated to a moving object, the Doppler effect increases the frequency of the reflected wave when the object approaches. The frequency of the reflected wave also decreases when the object moves away. As presented in Fig. 1, the blood flow velocities can be measured by irradiating the ultrasound wave from the body surface towards the blood vessels and observing the reflected waves from the red blood cells in the flowing blood. The radial artery and carotid artery, which are located near the skin, are suitable for the measurements.

The received frequency f_1 in the blood and the received frequency f_2 at the sensor device can be expressed as (3) and (4).

$$f_1 = \frac{c + \mathrm{v}\cos\theta\cos\alpha}{c} f_0 \quad \textbf{(3)}$$

$$f_2 = \frac{c}{c - v\cos\theta\cos\alpha} f_1 \quad \textbf{(4)}$$

Here, f_0, c, and v denote the transmitted frequency, in vivo sound velocity [m/s], and blood flow velocity [m/s], respectively. In those equations, θ and α denote the irradiation angle between the ultrasound wave and the blood flow direction, respectively, as depicted in Fig. 6. Because $v \ll c$ in vivo, f_2 can be expressed as

$$\begin{aligned} f_2 &= \frac{c + v\cos\theta\cos\alpha}{c - v\cos\theta\cos\alpha} f_0 \\ &\approx \left(1 + \frac{2v\cos\theta\cos\alpha}{c}\right) f_0. \end{aligned} \quad \textbf{(5)}$$

Consequently, the Doppler-shifted frequency f_d is

$$f_d = f_2 - f_0 = \frac{2v\cos\theta\cos\alpha}{c} f_0. \quad \textbf{(6)}$$

The blood flow velocity is calculable as shown below.

$$v = \frac{c}{2\cos\theta\cos\alpha} \frac{f_d}{f_0} \quad \textbf{(7)}$$

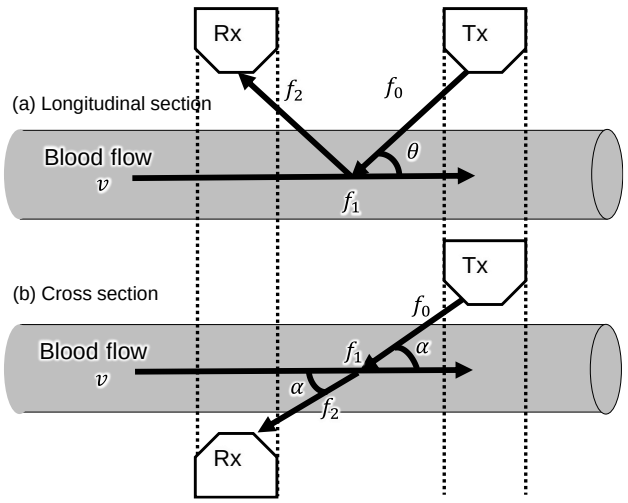

Figure 6 Angle between ultrasound wave and blood flow.

The transmitted wave Tx(t) and the received wave Rx(t) can be expressed as (8) and (9), respectively.

$$\mathrm{Tx}(t) = \sin(2\pi f_0 t) \quad \textbf{(8)}$$

$$\mathrm{Rx}(t) = \sin(2\pi(f_0 + f_d)t) \quad \textbf{(9)}$$

The shifted frequency component can be extracted by mixing Tx and Rx. The mixed output I(t) is

$$\begin{aligned} \mathrm{I}(t) &= \mathrm{Tx}(t) \times \mathrm{Rx}(t) \\ &= \sin(2\pi f_0 t) \times \sin(2\pi(f_0 + f_d)t) \\ &= \frac{1}{2}\{\cos(2\pi(f_0 + f_d)t - 2\pi f_0 t) \\ &\qquad - \cos(2\pi(f_0 + f_d)t + 2\pi f_0 t)\} \\ &= \tfrac{1}{2}\{\cos(2\pi f_d t) - \cos(2\pi(2f_0 + f_d)t)\}. \end{aligned} \quad \textbf{(10)}$$

The high-frequency component of the second term of (10) is removed by the low-pass filter as (11).

$$\begin{aligned} \mathrm{I}(t) &= \frac{1}{2}\cos(2\pi f_d t) \\ &= \frac{1}{2}\left\{\sin\left(2\pi f_d t + \frac{\pi}{2}\right)\right\} \end{aligned} \quad \textbf{(11)}$$

In this study, a 40-kHz ultrasound is used to measure the blood flow velocity. However, because the amount of frequency shift caused by the Doppler effect is proportional to the frequency of the transmitted wave, a frequency analysis technique that captures an extremely low frequency shift is necessary. Assuming that the range of the blood flow velocity is 1–30 [cm/s], the frequency shift with respect to the ultrasound wave of 40 kHz is from 1 to 20 Hz.

To observe this frequency shift, at least a few seconds of window length is required. The frequency analysis resolution depends on the sampling frequency and window width. However, it is necessary to limit the window width to several hundred milliseconds to achieve a higher time resolution and to observe changes in the blood flow rate with each heartbeat.

When assuming the FFT with 100-kHz sampling frequency and 0.1 s window width, its frequency resolution is 10 Hz. Therefore, a frequency analysis method using an autoregressive (AR) model is chosen in this study instead of the FFT. The AR-model-based method has a higher frequency resolution, even with a small window width.

The AR model of time series $x(t)$ is expressed as (12).

$$x(t) = \sum_{m=1}^{M} a(m)x(t-m) + e(t) \quad \textbf{(12)}$$

Here, a, e, and Mdenote the AR coefficient, white noise, and the order of the model, respectively.

The Berg method, which is used for the parameter estimation of the AR model [12], obtains the parameters by minimizing the forward prediction error and the backward prediction error of the data. The least-squares method is used

for the evaluation function. Frequency analysis using the Burg method exhibits sharper frequency peaks even with the same window length compared to the FFT [13].

The power spectrum density is calculable from (13) according to the AR model parameters.

$$P(f) = \frac{1}{F_s} \frac{\sigma^2}{|1 - \sum_{m=1}^{M} a(m) e^{-j2\pi i f / F_s}|} \quad \textbf{(13)}$$

Here, F_s and σ^2 denote the sampling frequency and deviation of white noise e, respectively. The order M is set empirically to 10 in this study.

C. Measurement Method of PWV

PWV is the time difference until a pulse wave reaches the blood vessels at two arbitrary points. The conventional method measures it using multiple devices, such as ECG and PPG at the fingertips, or two pulse waves at the wrist and ankle. These distances are separated by tens of centimeters or more. In contrast, the proposed method estimates the PWV by placing two piezoelectric transducers separated by a distance of 1–2 cm, and measuring the phase difference in the pulse wave (see Fig. 7).

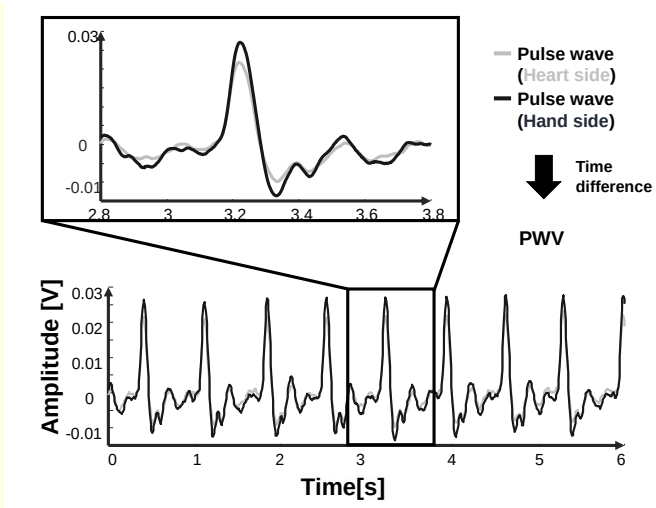

Figure 7 Measurement example of pulse waves.

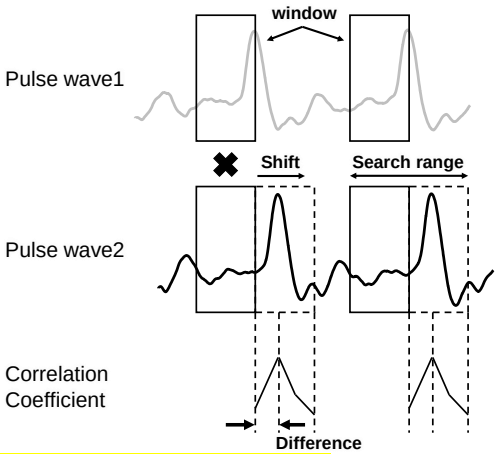

Figure 8 Autocorrelation of pulse wave.

Because of the short distance between the piezoelectric transducers, the difference in the pulse wave arrival times becomes smaller than that obtained by the conventional method. The difference in arrival time is almost proportional to the distance. Moreover, because the pressure pulse waves are measured on the skin surface as described above, it is susceptible to noise influences such as body movements. Therefore, it is difficult to obtain the PWV from the time difference in the pulse wave only using the peak time information.

To overcome this difficulty, we introduce two methods. First, the proposed method calculates a cross correlation similarly as the heartbeat extraction as described in Section III.A and [10]. After the autocorrelation is used for heartbeat extraction, the cross correlation is calculated between two measured pulse wave signals to extract the PWV. The cross correlation is calculated while shifting the two pulse waves (see Fig. 8). The shift width that maximizes the correlation coefficient is sought. Then, the proposed method calculates the correlation with the rising part of the pressure pulse wave, because the pressure pulse wave includes a reflected wave as shown in Fig. 9. The reflected wave component is included in the falling part of the measured wave. The progressive wave component and the reflected wave component move in the opposite direction in proportion to the PWV. Only the influence of the progressive wave is evaluated by calculating the correlation from only the rising part.

D. Implementation of prototype

The prototype of the proposed method is implemented as

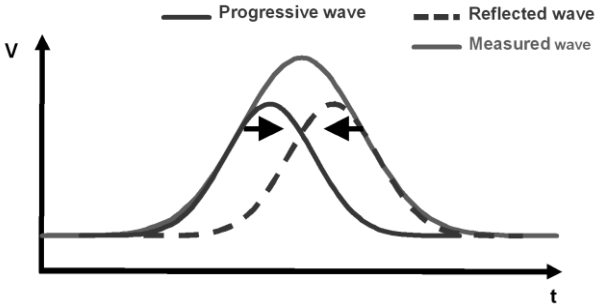

Figure 9 Progressive wave and reflected wave in pulse wave.

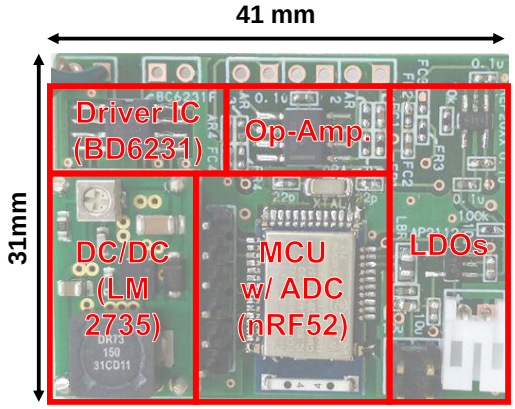

Figure 10 PCB of prototype sensor.

shown in Figs. 10, 11, and 12. The PCB shown in Fig. 10 consists of LDOs, a DC/DC converter, a driver IC, two op-amps, and a MCU with an AD converter. A battery and

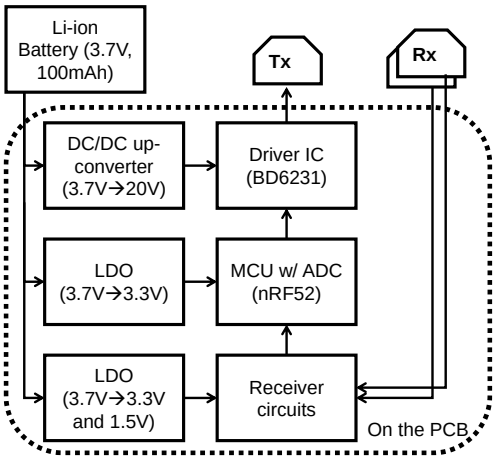

Figure 11 Block diagram of prototype sensor.

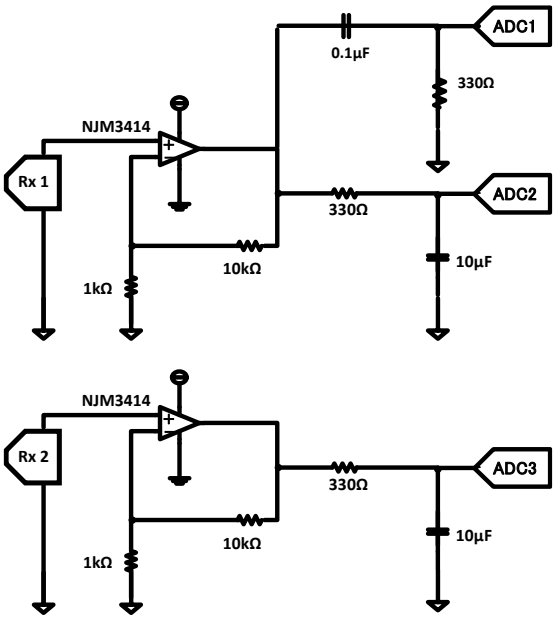

Figure 12 Receiver circuits.

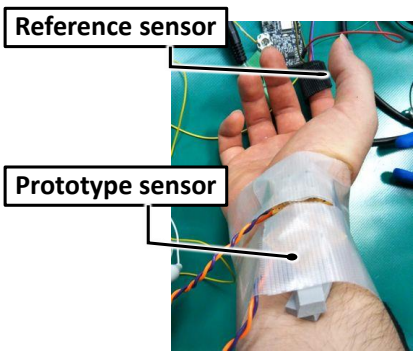

Figure 13 Experimental setup.

piezoelectric transducers are externally connected to this PCB, as shown in Fig. 11. The receiver circuit is composed of two op-amps. After amplifying the received signal, the Doppler waves and pulse waves are separated by the filters. The Doppler shift frequency can be measured by under sampling using the AD converter. Thus, the signal frequency of the difference between the sampling frequency and the input frequency can be obtained, and the same signal as that from mixing can be obtained.

IV. Measurement Results

Measurement and performance evaluations are conducted using the proposed sensor device to examine two male participants who are 23 and 33 years old. The measurement is conducted at the rest condition. Fig. 13 shows our experimental setup. Two PPG sensors and an ECG sensor are used as the reference.

First, the accuracy of the heartbeat interval is evaluated. Fig. 14 presents a comparison of heart rates that is extracted by the proposed pulse wave sensor with autocorrelation and the reference ECG. According to the correlation coefficient and its maximum value, the RMS errors of two measured results are suppressed to 0.83 bpm and 0.74 bpm, respectively. .

Next, the PWV is evaluated. Fig. 15 shows the relation between the arrival time difference measured by the proposed sensor and the reference PPG sensors. The reference PPG sensors are set to the fingertip and elbow of the participant. The measurement result shows that the correlation coefficient

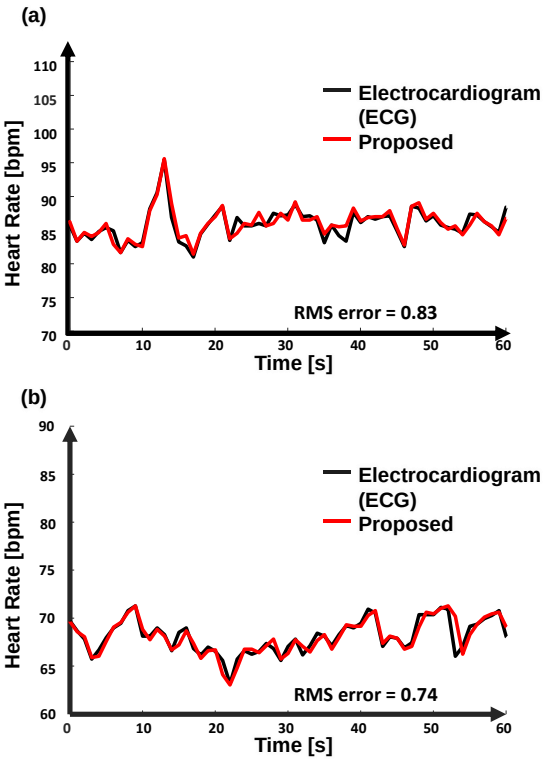

Figure 14 Comparison of measured heart beat interval: (a) subject #1 and (b) subject #2.

r is 0.738 and 0.727, indicating a positive correlation. In Fig. 15(b), the time difference between proposed pulse waves has negative value. This result is caused by the difference of heart beat waveform in two pulse waves.

Finally, the blood flow velocity is evaluated as shown in Fig. 16. Fig. 16(a) presents the measured Doppler wave with 40-kHz under sampling. Fig. 16(b) shows the result of the frequency analysis using the proposed method described in Section IIIb. Fig. 16(c) and Fig. 16(d) shows the result of another participant. Although the waveform has different shape in the time domain because the positional relationship between the sensor and blood vessel is different, the blood flow at the time of stroke is correctly captured in the frequency domain. The measurement result shows that changes in the blood flow velocity of each beat can be measured. However, the absolute value of the speed is lower than the actual value because the angle between the piezoelectric transducer and the blood vessel deviated from the assumed value. We anticipate this problem to be solvable by beamforming using a piezoelectric transducer array, which is a task for future work.

The measured current consumption was less than 100 μA on average for the receiving sensor and microcontroller, and 35 mA on average for the ultrasound transmitter including DC/DC converter.

V. Conclusion

As described herein, we proposed a multimodal cardiovascular information sensing method for wearable healthcare. In this study, two pulse waves: the pulse wave and blood flow velocity were measured, separately. Our measurement results showed that the prototype sensor could extract each information correctly. This demonstrated the possibility of the simultaneous measurement of pulse wave, pulse transit time, and blood flow velocity.

Future development tasks are power reduction and measurement accuracy improvement. Although the transmitting power is dominant, it can be reduced by intermittent operation. In addition, the position of the sensor device relative to the body surface and the influence of individual differences in the human hands should be considered. For miniaturization, we are considering the application of a flexible sensor array using a piezoelectric film rather than piezoceramic. An effective method of improving the accuracy is increasing the number of sensor arrays to perform beam forming.

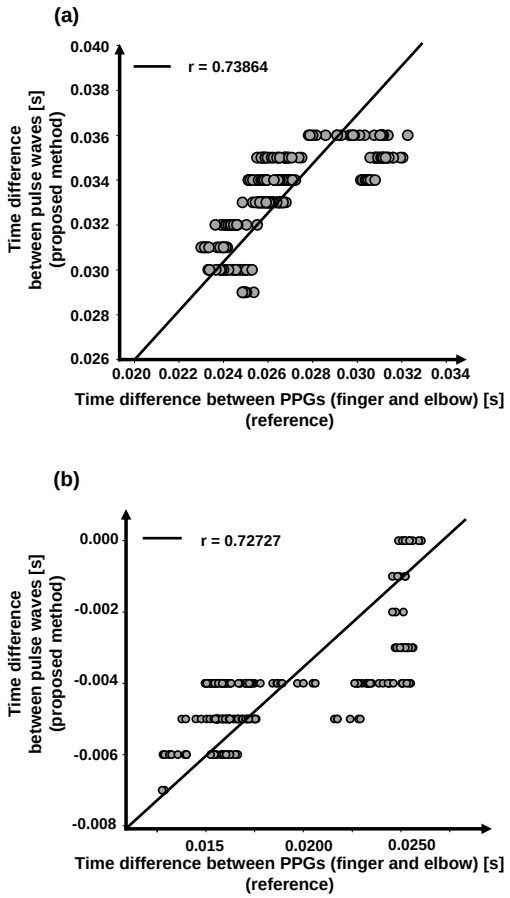

Figure 15 Correlation of arrival time difference between piezoerectric trancducers and PPG(Finger) to PPG(Elbow): (a) subject #1 and (b) subject #2.

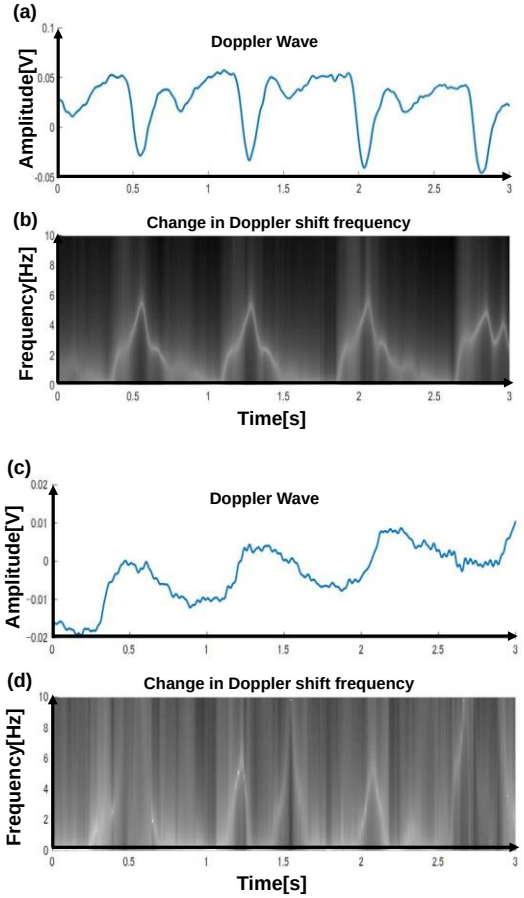

Figure 16 Measurement result of blood flow velocity: (a) subject #1 (time domain), (b) subject #1 (frequency domain), (c) subject #2 (time domain), and (d) subject #2 (frequency domain).

References

[1] Ya-Li Zheng. (2014). Unobtrusive Sensing and Wearable Devices for Health Informatics, in *Proc. of IEEE Transactions on Biomedical Engineering* , Vol. 61, No. 5, pp.1538-1554, May.

[2] S. Seneviratne et al. (2017). A Survey of Wearable Devices and Challenges, in *IEEE Communications Surveys & Tutorials*, vol. 19, no. 4, pp. 2573-2620

[3] T. Liang and Y. J. Yuan. (2016). Wearable Medical Monitoring Systems Based on Wireless Networks: A Review, in *IEEE Sensors Journal*, vol. 16, no. 23, pp. 8186-8199, Dec.

[4] S. M. R. Islam, D. Kwak, M. H. Kabir, M. Hossain and K. Kwak. (2015). The Internet of Things for Health Care, in *IEEE Access*, vol. 3, pp. 678-708.

[5] L. Sornanathan and I. Khalil. (2010). Fitness monitoring system based on heart rate and SpO2 level, in *Proc. of IEEE ITAB*, Nov.

[6] M. V. Kamath, M. A. Watanabe, and A. R..M. Upton. (2012). *Heart Rate Variability(HRV) Signal Analysis CLINICAL APPLICATIONS*, CRC Press.

[7] S. Shukla. (2015). Noninvasive cuffless blood pressure measurement by vascular transit time, *VLSI Design (VLSID)*, pp. 535-540.

[8] A. H. Khandoker, V. Luthra, Y. Abouallaban, S. Saha, K. I. Ahmed, R. Mostafa, N. Chowdhury, and H. F. Jelinek. (2015). Reduced variability in pulse wave velocity in depressed patients with suicidal ideation, in *Proc. Computing in Cardiology Conference (CinC)*, Sept.

[9] H. Takeuchi and N. Kodama. (2017). Time-series data analysis of home blood flow velocity measurement from radial artery in relation to lifestyle factors, in *Proc. IEEE BHI*, Feb.

[10] Y. Nakai, S. Izumi, M. Nakano, K. Yamashita, T. Fujii, H. Kawaguchi, and M. Yoshimoto. (2014). Noise tolerant QRS detection using template matching with short-term autocorrelation, in *Proc. of IEEE EMBC*, pp. 34-37, Aug.

[11] K. Saito, M. Nishihira, and K. Imano. (2006). Design and experimental study on acoustic properties of (0-3) composite materials for acoustic matching layer of air-coupled ultrasound transducer, *Journal of the Society of Materials Engineering for Resources of Japan*, vol. 19, no. 1-2, pp. 11-17.

[12] K. Vos. (2013). A fast implementation of Burg`s method, www.opus-codec.org/docs/vos_fastburg.pdf, Aug..

[13] D. Matsunaga, S. Izumi, H. Kawaguchi, and M. Yoshimoto. (2016). Non-contact instantaneous heart rate monitoring using microwave doppler sensor and time-frequency domain analysis, in *Proc. of IEEE BIBE*, pp. 172-175, Oct.

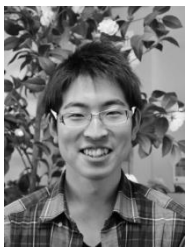

Takaaki Okano received his B.Eng. degree in Computer and Systems Engineering from Kobe University, Hyogo, Japan, in 2017. Currently, he is a master course student at Kobe University. His current research is related to wearable healthcare systems.

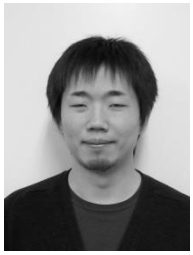

Shintaro Izumi respectively received his B.Eng. and M.Eng. degrees in Computer Science and Systems Engineering from Kobe University, Hyogo, Japan, in 2007 and 2008. He received his Ph.D. degree in Engineering from Kobe University in 2011. He was a JSPS research fellow at Kobe University from 2009 to 2011, and an Assistant Professor in the Organization of Advanced Science and Technology at Kobe University from 2011 to 2018. Since 2018, he has been an Associate Professor in the Institute of Scientific and Industrial Research, Osaka University, Japan. His current research interests include biomedical signal processing, communication protocols, low-power VLSI design, and sensor networks.
He has served as a Chair of IEEE Kansai Section Young Professionals Affinity Group, as a Technical Committee Member for IEEE Biomedical and Life Science Circuits and Systems, as a Student Activity Committee Member for IEEE Kansai Section, and as a Program Committee Member for IEEE Symposium on Low-Power and High-Speed Chips (COOL Chips). He was a recipient of 2010 IEEE SSCS Japan Chapter Young Researchers Award.

Takumi Katsuura received his B.Eng. degree in Computer and Systems Engineering from Kobe University, Hyogo, Japan, in 2017. Currently, he is a master course student at Kobe University. His current research is related to wearable healthcare systems.

Hiroshi Kawaguchi received his B.Eng. and M.Eng. degrees in electronic engineering from Chiba University, Chiba, Japan, in 1991 and 1993, respectively, and his Ph.D. degree in Engineering from The University of Tokyo, Tokyo, Japan, in 2006.
He joined Konami Corporation, Kobe, Japan, in 1993, where he developed arcade entertainment systems. He joined The Institute of Industrial Science, The University of Tokyo, as a Technical Associate in 1996, and was appointed as a Research Associate in 2003. In 2005, he joined Kobe University, Kobe, Japan. Since 2007, he has been an Associate Professor with The Department of Information Science at the university thereof. He is also a Collaborative Researcher with The Institute of Industrial Science, The University of Tokyo. His current research interests include low-voltage SRAM, RF circuits, and ubiquitous sensor networks.
Dr. Kawaguchi was a recipient of the IEEE ISSCC 2004 Takuo Sugano Outstanding Paper Award and the IEEE Kansai Section 2006 Gold Award. He has served as a Program Committee Member for IEEE Custom Integrated Circuits Conference (CICC) and IEEE Symposium on Low-Power and High-Speed Chips (COOL Chips), and as a Guest Associate Editor of the IEICE Transactions on Fundamentals of Electronics, Communications and Computer Sciences, and IPSJ Transactions on System LSI Design Methodology (TSLDM).

Masahiko Yoshimoto joined the LSI Laboratory, Mitsubishi Electric Corporation, Itami, Japan, in 1977. From 1978 to1983, he had been engaged in the design of NMOS and CMOS static RAM. Since 1984, he had been involved in the research and development of multimedia ULSI systems. He earned a Ph.D. degree in Electrical Engineering from Nagoya University, Nagoya, Japan in 1998. Since 2000, he had been a professor of the Department of Electrical & Electronic System Engineering in Kanazawa University, Japan. Since 2004, he has been a professor of the Department of Computer and Systems Engineering in Kobe University, Japan. His current activity is focused on the research and development of an ultralow power multimedia, ubiquitous media VLSI systems, and a dependable SRAM circuit. He holds 70 registered patents. He has served on the program committee of the IEEE International Solid State Circuit Conference from 1991 to 1993. Additionally, he served as a Guest Editor for special issues on Low-Power System LSI, IP, and Related

Technologies of IEICE Transactions in 2004. He was a chair of the IEEE SSCS (Solid State Circuits Society) Kansai Chapter from 2009 to 2010. He is also a chair of the IEICE Electronics Society Technical Committee on Integrated Circuits and Devices from 2011–2012. He received the R&D100 awards from the R&D magazine for the development of the DISP and the development of the real-time MPEG2 video encoder chipset in 1990 and 1996, respectively. He also received the 21th TELECOM System Technology Award in 2006.